Cover Page

Fill out and attach to your manuscript — DUE Monday, November 16, 2020

The 29th International Toki Conference (ITC-29)

Presentation Number:	P1-F2-6
Paper Title:	Simulation of Impurity Transport and Deposition in the Closed Helical Divertor in the Large Helical Device Using ERO2.0
Corresponding Author:	Mamoru SHOJI
Affiliation:	National Institute for Fusion Science
Full Postal Address:	322-6 Toki, Gifu 509-5292, Japan
Telephone:	+81-572-58-2151
Fax:	+81-572-58-2618
E-mail:	shoji@nifs.ac.jp
Topic Category in ITC-29 (see the list below)	(1)

LIST OF TOPICS CATEGORY in ITC-29

(1) Magnetically Confined Plasmas
(2) Inertially Confined Plasmas
(3) Fusion Engineering and Reactor Design
(4) Basic Plasma Research and Plasma Application
(5) Fundamental Theory and Simulation Techniques
(6) Space and Astrophysical Plasmas
(7) Data Driven Plasma Science
(8) Special Session on “Steady State Operation of Magnetically Confined Plasmas”

Notes:

- **Above categories are not in one-to-one correspondence with the 6 topics in the submission site of PFR. Please choose a topic which is mostly related to your article when you submit a paper on PFR online submission site.**

Simulation of Impurity Transport and Deposition in the Closed Helical Divertor in the Large Helical Device

Mamoru SHOJI[1)], Gakushi KAWAMURA[1,2)], Juri ROMAZANOV[3)], Andreas KIRSCHNER[3)], Alina EKSAEVA[3)], Dmitry BORODIN[3)], Suguru MASUZAKI[1,2)], and Sebastijan BREZINSEK[3)]

1) National Institute for Fusion Science, National Institutes of Natural Sciences, 322-6 Oroshi-cho, Toki 509-5292, Japan

2) The Graduate University for Advanced Studies (SOKENDAI), Shonan Village, Hayama 240-0913, Japan

3) Forschungszentrum Jülich GmbH, Institut für Energie- und Klimaforschung - Plasmaphysik, Partner of the Trilateral Euregio Cluster (TEC), Jülich 52425, Germany

Long pulse discharges in the Large Helical Device have often been interrupted by large amounts of dust particle emission from the divertor region caused by the exfoliation of carbon-rich mixed material deposition layers. The plasma wall interaction code ERO2.0 has provided the simulation results of the three-dimensional distribution of the carbon flux density in the divertor region which is quite reasonable with the observed density profiles of the carbon-rich deposition layers. The code has also succeeded in reproducing the significant reduction of the carbon deposition layers on dome plates by changing the target plate configuration in the divertor region. The ERO2.0 simulations have successfully explained dust particle emission near the equatorial plane in the new target plate configuration at the termination of a long pulse discharge. These simulation results prove that the ERO2.0 code is applicable to predicting the possible position of the dust particle emission, and to designing an optimized divertor configuration for stable long pulse discharges with controlled dust particle emission.

Keywords: ero2.0, plasma wall interactions, simulation, impurity transport, divertor, peripheral plasma, emc3-eirene, large helical device.

1. Introduction

The influence of dust particles in magnetic plasma confinement devices has recently gained attention from the viewpoint of the effect on the plasma performances. Long pulse plasma discharges in the Large Helical Device (LHD) provide unique opportunities for studying plasma-wall interactions under steady-state operation such as future nuclear fusion reactors [1]. Recently, it has been found that long pulse discharges in LHD are often interrupted by the large amounts of dust particle emission from the closed helical divertor region [2]. The traces of the exfoliation of carbon-rich mixed material deposition layers were found in the divertor region, which led to the interruption of the long pulse discharges due to radiation collapse caused by the impurities included in the dust particles. Two possible scenarios of the exfoliation of the deposition layers show that the thick carbon-rich layers are easily exfoliated from lower brittle iron-rich layers [3]. For controlling the exfoliation of the deposition layers, the distribution of the carbon flux density in the divertor region was analyzed using the Monte-Carlo based three-dimensional plasma wall interaction simulation code ERO2.0 [4]. This analysis can contribute to sustaining long pulse discharges with reduced dust particle emission by controlling the carbon flux density in the divertor region.

2. Interruption of long pulse discharges by dust particle emission from the divertor region

In the experimental campaign in fiscal year (FY) 2013, a long pulse discharge has been successfully sustained for approximately 48 minutes in LHD. The termination process of this plasma discharge was observed with a fast framing camera, which revealed that the plasma was interrupted by radiation collapse induced by emission of the large amounts of dust particles from the closed helical divertor region [2]. After this experimental campaign, the traces of the exfoliation of deposition layers were found on the surface of dome plates in the divertor region as shown in Figure 1 (a). This image indicates that the dust particles were released by the exfoliation of the deposition layers on the dome plates. In the closed helical divertor, target plates, which are installed at both upper and lower ends of the divertor region, directly intersect the LHD divertor plasma, and the front surface of the target plates directly faces toward the dome plates. These two locally enhances the carbon deposition on the dome plates installed in front of

author's shohji.mamoru@nifs.ac.jp

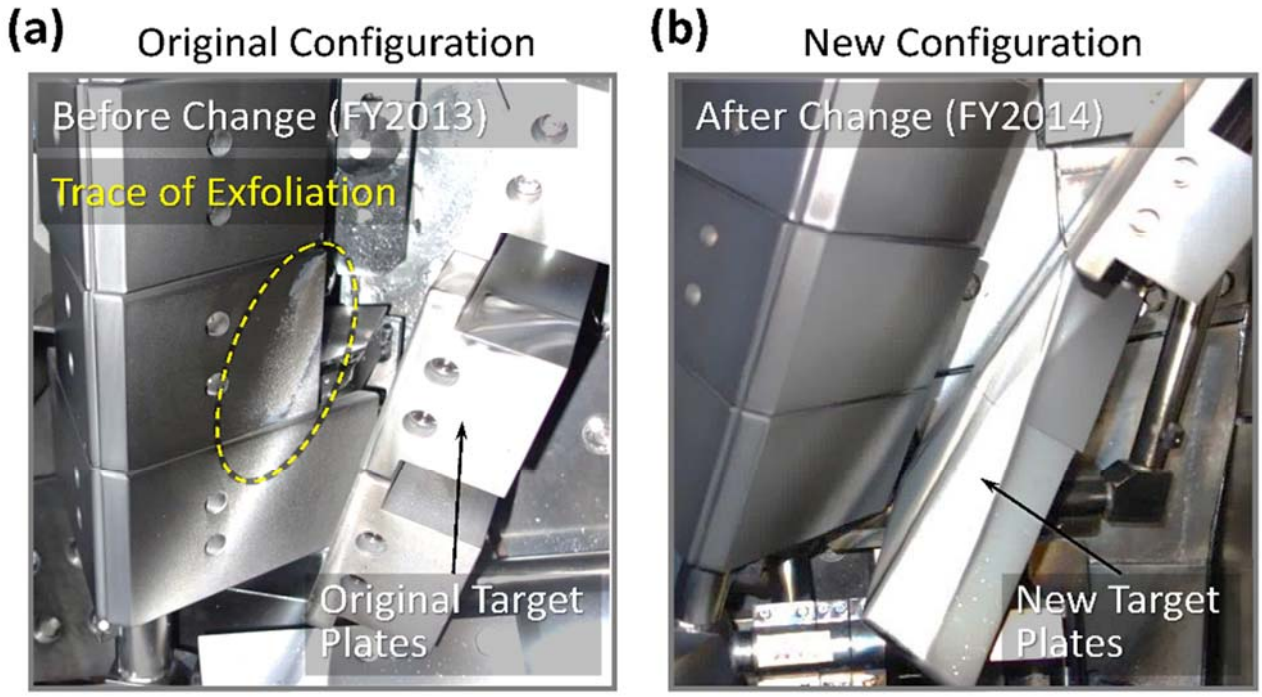

Fig.1 The image -of the carbon-rich mixed material deposition layers on the dome plates in front of the target plates in the original target plate configuration in FY2013 (a) and that in the new target plate configuration in FY2014 (b).

the target plates by physical and chemical sputtering on the target plates [5].

In order to control the carbon deposition on the dome plates, the configuration of the target plates was changed after the experimental campaign in FY 2013 (before FY 2014) such that the front surface of the target plates directly faces toward the main plasma (not to the dome plates). Due to the change, the deposition of the sputtered carbon on the dome plates is reduced, which led to that long pulse discharges in FY2014 were not interrupted by dust particle emission from the dome plates near the target plates. No traces of the exfoliation of the deposition layers were found in the divertor region in this experimental campaign (FY2014) as shown in Figure 1 (b).

3. Setup of the grid model of the closed helical divertor for the ERO2.0 simulation

The three-dimensional plasma-wall interaction simulation code ERO2.0 was applied to investigate the effect of the change of the target plate configuration on the distribution of the carbon flux density on the dome plates in the closed helical divertor region. Figure 2 (a) illustrates the perspective view of the three-dimensional grid model for the simulation. This model includes plasma facing components (PFMs) such as the divertor components (dome and divertor plates) and the vacuum vessel in one helical coil pitch angle (36° in toroidal direction). The surfaces of the divertor components and the vacuum vessel are treated as carbon and iron, respectively. These components consist of aggregates of many small triangle surfaces which size is in the order of a few centimeters. The poloidal planes at both two toroidal edges are treated as periodic boundaries. Two grid models were prepared for simulating the closed helical divertor configuration before and after the change of the target plates. These are named as original and new target plate configurations, respectively. Figure 2 (b) and (c) display the enlarged figures of the grid model for the original and new configurations, respectively.

The fixed three-dimensional background (BG) plasma for the ERO2.0 simulation is provided by a three-dimensional edge plasma simulation code (EMC3-EIRENE) [6, 7]. The parameter profile in the BG plasma is the calculation by this code in the case where the plasma heating power P^{LCFS} and the plasma density n_e^{LCFS} at an inner boundary of the calculation domain just inside of the LCFS (Last Closed Flux Surface) are set to be 8 MW and 8 $\times 10^{19}$ m^{-3}, respectively. The magnetic configuration is set to be the most typical configuration where the radial position of the magnetic axis R_{ax} is 3.60 m, and the toroidal magnetic field direction is clockwise. The perpendicular particle and the ion/electron thermal diffusion coefficients of the BG plasma are assumed to be 0.5 and 1.0 m^2/s, respectively, which are typical values for explaining the measured electron temperature and density profiles in the LHD peripheral plasma.

In the ERO2.0 code, many test particles (in the order

author's shohji.mamoru@nifs.ac.jp

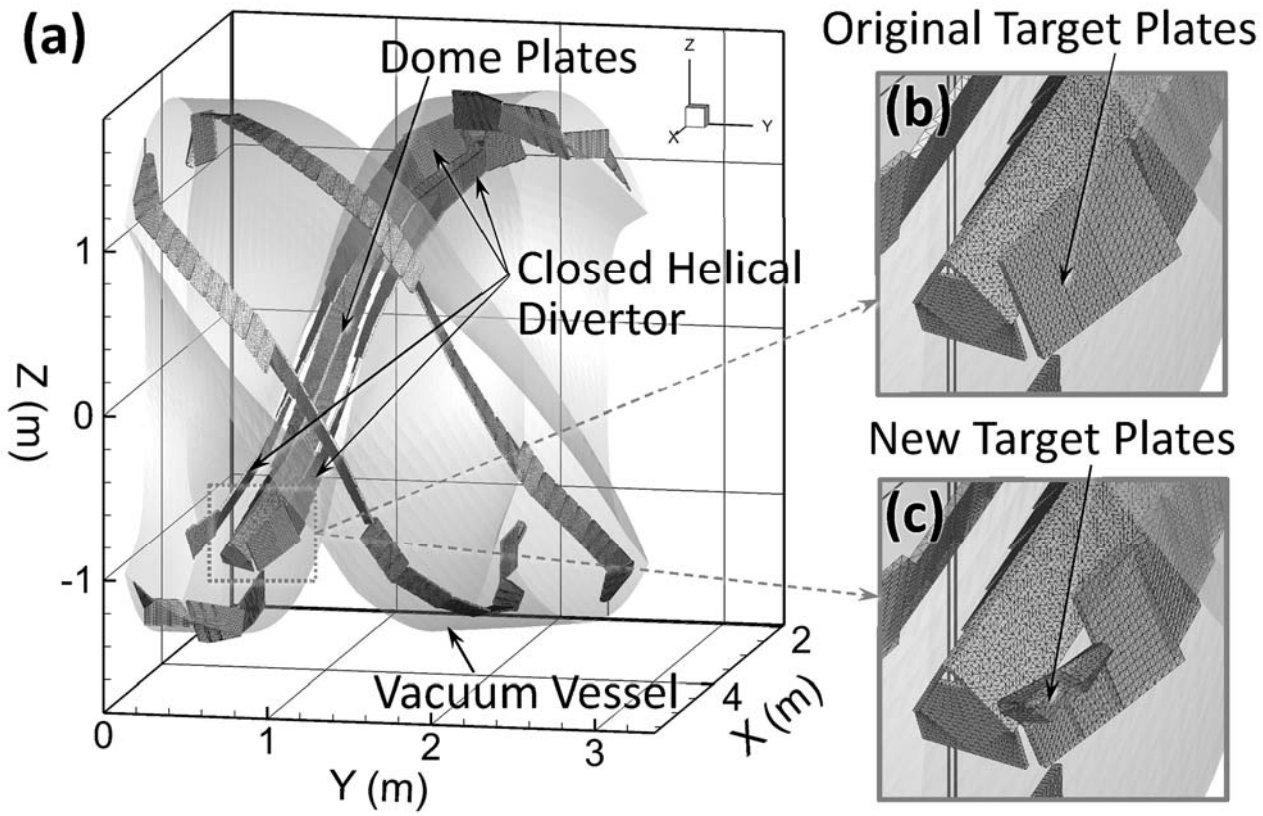

Fig.2 The perspective view of the three-dimensional grid model for the ERO2.0 simulation (a). The enlarged figures of the model for the original target plate configuration (b) and the new target plate configuration (c).

of several ten million), which are representative of carbon atoms or hydrocarbon molecules, are launched from the strike points on the divertor plates. These are produced by physical and chemical sputtering on the divertor plates due to the incident deuterium ions in the divertor plasma. The ionization/recombination rates of carbon atoms/ions and hydrocarbon molecules are derived from the database on the Atomic Data and Analysis Structure (ADAS) [8]. The ERO2.0 code tracks carbon ion trajectories in the plasma with a diffusion coefficient of 1.0 m^2/s which provides reasonable simulation results being compatible with both observed carbon line emission ratios and the absolute line emission [9]. When the test particles (carbon ions) enter the inner boundary of the grid model, new test particles are regenerated at random positions on the surface at the inner boundary. This is an adequate measure for simulating the impurity transport in the core plasma because of the formation of the nested magnetic flux surfaces in this region.

4. The ERO2.0 simulation of the carbon flux density in the closed helical divertor

In the ERO2.0 simulation, carbon atoms (ions) and hydrocarbon molecules (molecular ions) colliding with the PFMs are deposited on or reflected from the surfaces of the PFMs. These particles also induce the physical and chemical sputtering on the PFMs. The angular and energy dependences of the reflection coefficients and sputtering yields of the particles are calculated using the database of the calculations by PWI simulation codes such as SDTrimSP [9]. The erosion of the deposited carbon induced by the BG plasma (deuterium ions) and by the sputtered carbon atoms released from the PFMs is not included in this simulation. The re-deposition of the eroded carbon and the carbon self-sputtering are also not considered for the simple calculation, which means that this simulation corresponds to a so-called “the first-time step calculation” in ERO2.0.

Figure 3 (a) and (b) give the simulation results of the distribution of the carbon flux density on the dome plates in the closed helical divertor region for the original and the new target plate configuration, respectively. The simulations by the ERO2.0 code show the reduction of the carbon flux density by changing the target plate configuration, which is qualitatively consistent with the deposition profile of the carbon-rich layers shown in Figure 1 (a) and (b). This reduced carbon flux density is favorable for controlling the dust emission from the divertor region.

author's shohji.mamoru@nifs.ac.jp

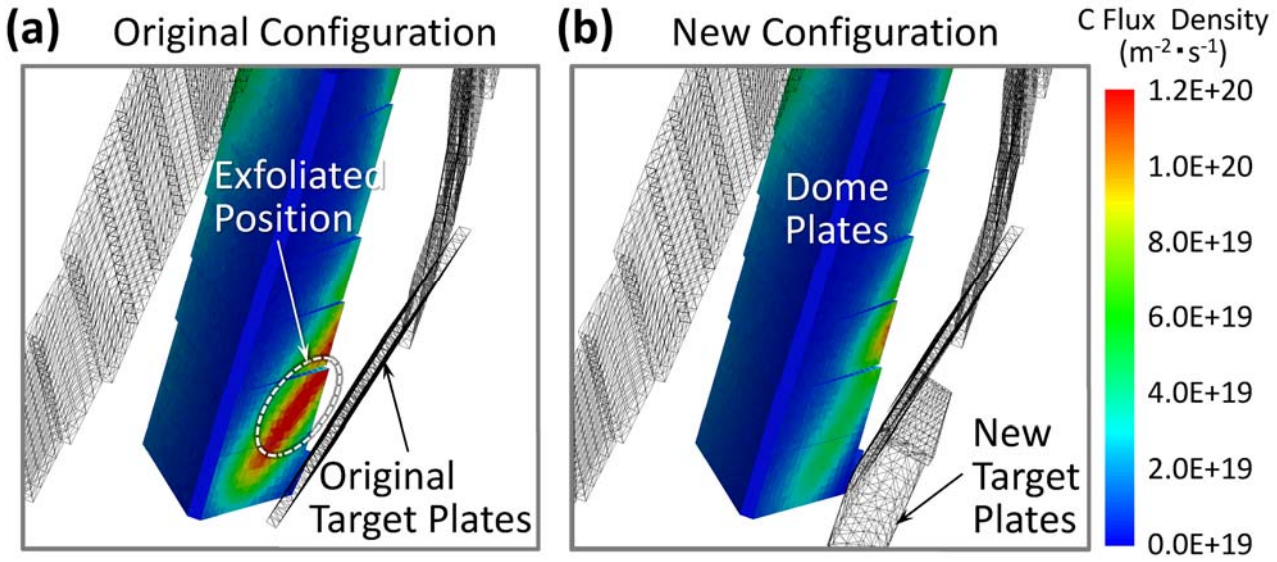

Fig.3 The simulations of the distribution of the carbon flux density on the dome plates in the closed helical divertor for the original target plate configuration (a) and the new target plate configuration (b).

The simulation for the original target plate configuration (Figure 3 (a)) shows that the area with the highest carbon flux density on the dome plates corresponds to the position where the traces of the exfoliation of the deposition layers were actually found after the experimental campaign in FY2013 (before the change of the target plate configuration). This fact means that the ERO2.0 code exactly predicts a possible position where the deposition layers are exfoliated in the plasma discharges.

5. Dust particle emission near the equatorial plane in the new target plate configuration

Long pulse discharges in FY2014 (in the new target plate configuration) were often interrupted by dust particle emission from the closed helical divertor region near the equatorial plane in the inboard side of the torus. Figure 4 gives the sequential images showing the interruption process of a long pulse discharge in the experimental campaign (FY2014). These images were taken with a CCD camera installed in an outer port (9-O) for monitoring the closed helical divertor installed in the inboard side of the torus. The observed images reveal that the long pulse discharge was terminated by the emission of the large amounts of dust particles released from the closed helical

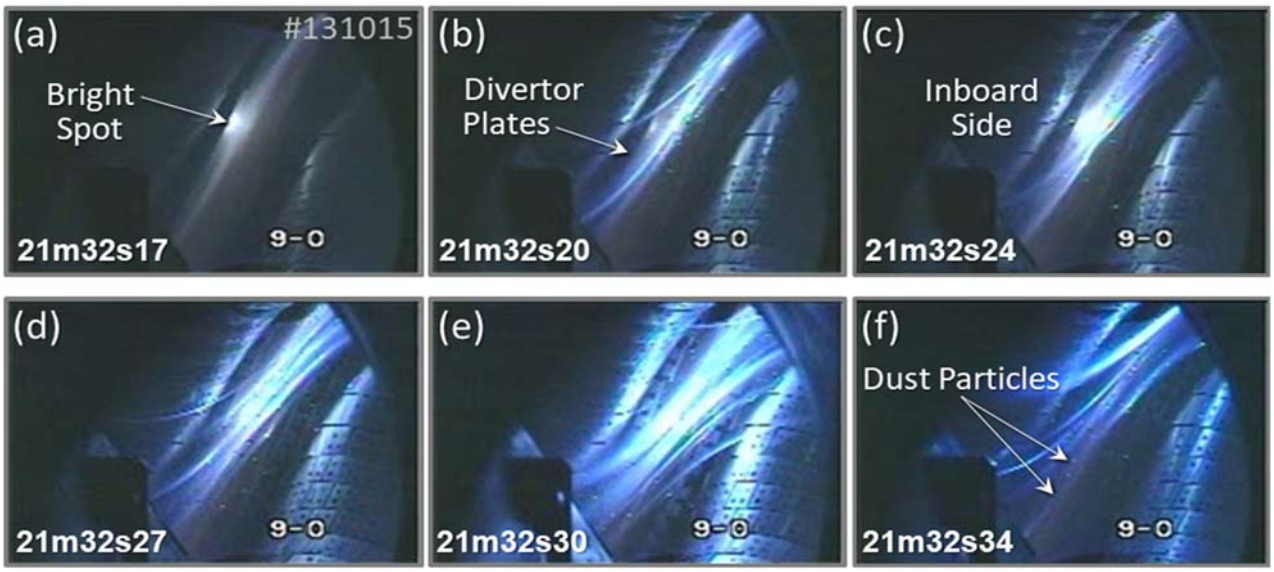

Fig.4 The sequential images showing the interruption process of a long pulse discharge in the experimental campaign (FY2014).

author's shohji.mamoru@nifs.ac.jp

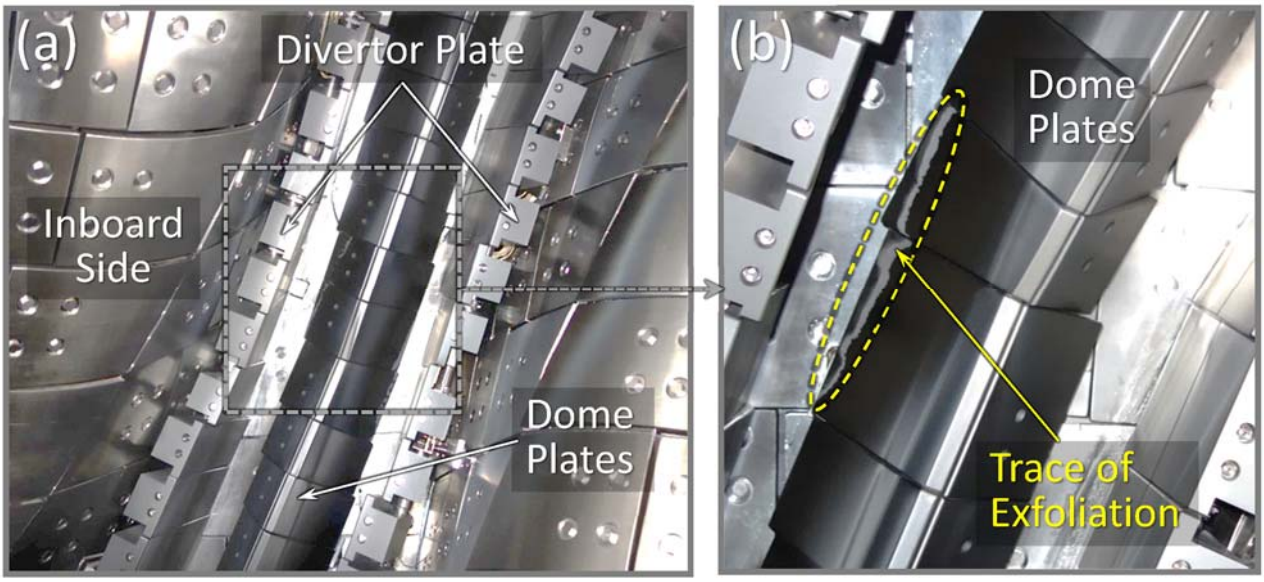

Fig.5 The images of the exfoliated carbon-rich deposition layers at the edge of the dome plates near the equatorial plane after the experimental campaign in FY2014 (in the new target plate configuration).

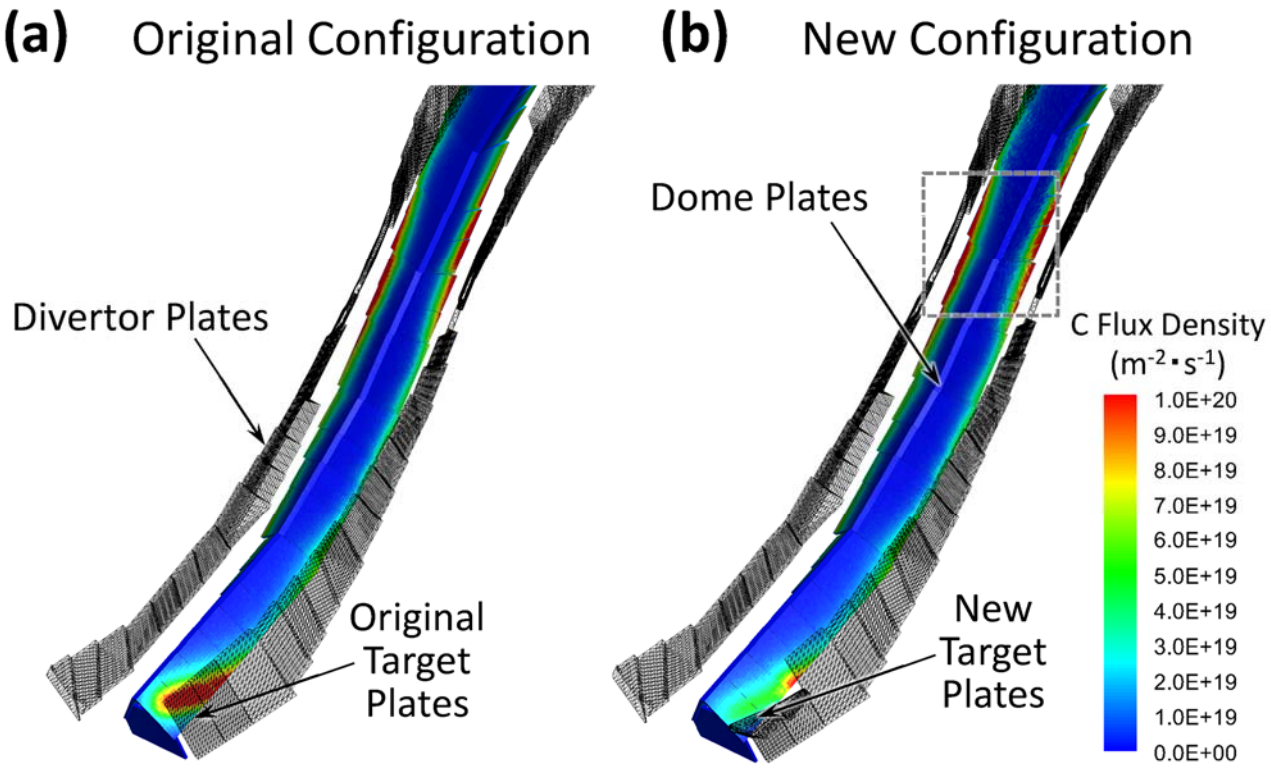

Fig.6 The ERO2.0 simulations of the carbon flux density distribution on the dome plates in the original target plate configuration (a) and in the new target plate configuration (b). The gray broken square in Figure (b) corresponds to the position of the image area in Figure 5 (b).

divertor region. As shown in Figure 4 (a), the plasma termination was triggered with a bright spot at a position near the equatorial plane in the inboard side.

After the experimental campaign in FY2014, the traces of the exfoliation of the carbon-rich deposition layers were found on the surface at the edge of the dome plates installed near the equatorial plane as shown in Figure 5 (a) and (b). This exfoliated area exactly agrees with the position where the bright spot was observed with the CCD camera just before the termination of the long pulse

author's shohji.mamoru@nifs.ac.jp

discharge (shown in Figure 4 (a)).

For investigating the reason for the dust particle emission from the divertor region near the equatorial plane in the new target plate configuration, the ERO2.0 simulations of the three-dimensional distribution of the carbon flux density on the dome plate are compared in the original and the new target plate configurations. Figure 6 (a) and (b) display the perspective view of the carbon flux density distribution on the dome plates in the original and new target plate configurations, respectively. In the original target plate configuration, the carbon flux density is maximum in front of the target plates as shown in the lower part in Figure 6 (a). The carbon flux density near the equatorial plane is the second highest in the original configuration. On the other hand, in the new target plate configuration, the carbon flux density is maximum at the edge of the dome plates near the equatorial plane, in which the carbon flux density in front of the target plates is significantly reduced in the new target plate configuration. These two simulations clearly show that the ERO2.0 simulations reasonably explain the position of the dust particle emission near the equatorial plane in the new target plate configuration. This is because thicker carbon-rich deposition layers are formed near the equatorial plane than in front of the target plates in this configuration.

6. Summary

Long pulse plasma discharges in the Large Helical Device have often been interrupted by the large amounts of dust particle emission from the closed helical divertor region by the exfoliation of the carbon-rich mixed material deposition layers. The Monte-Carlo based three-dimensional plasma wall interaction code ERO2.0 was applied to investigate the carbon flux density distribution in the divertor region. The simulations using ERO2.0 in a background plasma provided by EMC3-EIRENE have successfully reproduced the carbon flux density distribution on the dome plates in the closed helical divertor. In the original target plate configuration (in FY2013), the highest carbon flux density area obtained by the simulation exactly corresponds to the position where the exfoliation of the deposition layers was found. The simulation also reproduced the significant reduction of the carbon flux density on the dome plates in front of the target plates in the new configuration (in FY2014). After the change of the target plate configuration, long pulse discharges were often terminated by dust particle emission from the divertor region near the equatorial plane. This experimental result is reasonably explained by the ERO2.0 simulation which shows the highest carbon flux density at the edge of the dome plates near the equatorial plane. These experimental results prove that the ERO2.0 code is applicable to predicting the possible position of the dust particle emission, and to the design of an optimized divertor configuration for sustaining stable long pulse discharges with suppressed dust particle emission.

author's shohji.mamoru@nifs.ac.jp

Acknowledgments

This work is performed under the auspices of the NIFS Collaboration Research program (NIFS12KNXN236). One of the authors (M.S.) would like to thank Y. Feng for permission to use the EMC3-EIRENE. He also appreciates the computational resources of the LHD numerical analysis server and the plasma simulator in NIFS. This work is also supported by JSPS KAKENHI Grant Numbers 18H01203, 16H04619, and 16K18340.

References

[1] Y. Takeiri et al., Nucl. Fusion **57**, 102023 (2017).
[2] M. Shoji et al., Nucl. Fusion **55**, 053014 (2015).
[3] M. Tokitani et al., J. Nucl. Mater. **463**, 91 (2015).
[4] J. Romazanov et al., Nucl. Mater. Energy **18**, 331 (2019).
[5] M. Shoji et al., J. Nucl. Mater. **415**, S557 (2011).
[6] Y. Feng et al., Plasma Phys. Control. Fusion **44**, 611 (2002).
[7] G. Kawamura et al., Contrib. Plasma Phys. **54**, 437 (2014).
[8] The ADAS User Manual (version 2.6) http://adas.phys.strath.ac.uk/ (2004).
[9] S. Dai et al., Nucl. Fusion **56**, 066005 (2016).
[10] W. Möller et al., Comput. Phys. Commun. **51**, 355 (1988).